IOPscience iopscience.iop.org

Home Search Collections Journals About Contact us My IOPscience

An X-ray and nuclear magnetic resonance study of structure and ion motions in $(C(NH_2)_3)_3AlF_6$

This article has been downloaded from IOPscience. Please scroll down to see the full text article.

1992 J. Phys.: Condens. Matter 4 1837

(http://iopscience.iop.org/0953-8984/4/7/022)

View the table of contents for this issue, or go to the journal homepage for more

Download details:
IP Address: 171.66.16.159
The article was downloaded on 12/05/2010 at 11:18

Please note that terms and conditions apply.

J. Phys.: Condens. Matter 4 (1992) 1837–1848. Printed in the UK

An x-ray and nuclear magnetic resonance study of structure and ion motions in $[C(NH_2)_3]_3AlF_6$

M Grottel†, A Kozak, H Małuszyńska and Z Pająk
Institute of Physics, A Mickiewicz University, 60-780 Poznań, Poland
† Department of Physics, Academy of Agriculture, 60-637 Poznań, Poland

Received 1 March 1991, in final form 4 July 1991

Abstract. Guanidinium hexafluoroaluminate $[C(NH_2)_3]_3AlF_6$ crystallizes in a cubic system in the space group $P2_1/a\bar{3}$, $a = 13.953(2)$ Å, $Z = 8$. The guanidinium cation does not exhibit any symmetry; the hexafluoroaluminate anion has $\bar{3}$ symmetry and occupies two inequivalent (4a) and (4b) positions. The ions are connected by relatively strong N–H $\cdots$ F hydrogen bonds. Proton and fluorine spin–lattice relaxation times as well as second moments have been measured over a wide range of temperatures. The analysis of all cross-relaxation effects for the system of four unlike spins has been performed. Activation parameters for the C_3 reorientation of the cation and for the NH_2 group motion have been derived. Unlike in other guanidinium salts, anion reorientation is hindered by a much higher energy barrier than cation reorientation.

1. Introduction

This work is an extension of our x-ray and nuclear magnetic resonance (NMR) studies of crystal structures and ionic motions in various guanidinium salts. In all the compounds studied, the cation undergoes reorientation around its C_3 symmetry axis. The activation energy for this reorientation appears to depend on crystalline environment, reflecting H-bonding effects. We suggested the existence of additional amino group motion (Pająk *et al* 1982, Grottel and Pająk 1984), which was questioned by other authors (Gima *et al* 1984) or could not be confirmed (Ratcliffe 1985). In guanidinium tetrafluoroborate (Kozak *et al* 1987) and hexafluorophosphate (Grottel *et al* 1989) we described the dynamics of both the cation and anion sublattices by ^1H and ^{19}F NMR studies. To interpret the relaxation data we considered all cross-relaxation effects in the multi-spin systems. We succeeded in deriving the solution of the set of coupled differential equations describing the time variation of nuclear magnetizations for three and four unlike spins. It enabled us to extract precise activation parameters for the motions of both ions. Using these data we discovered a new effect: a convergence of rotational correlation times of the cations and anions at phase transitions (Pająk *et al* 1988). In guanidinium tetrafluoroborate and hexafluorophosphate, cation reorientation was preceded by isotropic anion reorientation, hindered by much lower energy barrier than cation reorientation.

To throw more light on the problem of cation and anion mobilities, we have chosen for the present investigation guanidinium hexafluoroaluminate $[C(NH_2)_3]_3AlF_6$, a 3 : 1 complex, interesting in relation to the 1 : 1 guanidinium complexes previously studied.

0953-8984/92/071837 + 12 $04.50 © 1992 IOP Publishing Ltd

In the case of hexafluoroaluminate we expected a higher energy barrier for the anion than for the cation. Each anion, being surrounded by three guanidinium ions, should be H-bonded much more strongly than in 1:1 complexes. We also presumed that it would be easier to detect the amino group motion, since a strong proton–fluorine interaction would be reduced by anion motion only at higher temperatures.

To determine the crystal structure of the compound first described by Bukovec (1983), we have undertaken its detailed x-ray analysis. In order to examine the dynamics of cation and anion sublattices, we studied proton and fluorine NMR second moments as well as spin–lattice relaxation times T_1 as a function of temperature. To interpret the complicated relaxation behaviour, we used the solution of the set of coupled differential equations describing the time variation of nuclear magnetizations for four unlike spins. To obtain further information on the ion dynamics, we analysed the temperature dependence of proton and fluorine magnetization amplitudes.

2. X-ray investigation

2.1. Crystal data

Guanidinium hexafluoroaluminate $[C(NH_2)_3]_3AlF_6$ crystallizes in a cubic system (from 40% aqueous HF) in space group $P2_1/a\bar{3}$, $a = 13.953(2)$ Å, $Z = 8$, $V = 2716.46$ Å^3, $M_w = 321.2$, $F(000) = 1328$, $\mu = 20.7$ cm^{-1}, $D_c = 1.571$ g cm^{-3}.

2.2. Experimental method

A crystal with dimensions of $0.3 \times 0.3 \times 0.4$ mm^3 was put on the Syntex $P2_1$ diffractometer with graphite-monochromated Cu K_α radiation ($\lambda = 1.5418$ Å). A total of 2198 reflections were collected ($h = 0$–15, $k = 0$–15, $l = 0$–15) up to $2\theta = 115°$ with variable scan, which averaged to 621 unique reflections, of which 584 were observed with $I > 1.96\sigma(I)$. No background measurements were made. The background and integrated intensities were obtained by the peak profile analysis method of Lehman and Larsen (1974) using the program PRARA (Jaskólski 1982). Corrections for Lorenz and polarization effects and empirical corrections for absorption effects were applied.

2.3. Structure determination and refinement

The structure has been solved by a direct method using the program SHELXS-86 (Sheldrick 1986), which revealed all non-hydrogen atoms. The hydrogen atom positions have been located on a difference Fourier map. The final full-matrix least-squares refinement of the positional and thermal parameters (anisotropic for non-hydrogen atoms, isotropic for hydrogen atoms) converged to

$$R = \sum |\Delta F| \Big/ \sum |F_0|$$

and

$$R_w = \left[\sum w(\Delta F)^2 \Big/ \sum w(F_0)^2 \right]^{1/2}$$

of 0.04 and 0.05 respectively, where $w = 1/[\sigma^2(F_0) + 0.0042F_0^2]$. The goodness of fit

$$S = \left[\sum w(\Delta F)^2/(N_O - N_V) \right]^{1/2}$$

was 1.09, where N_O is the number of observations and N_V is the number of parameters

Table 1. Fractional atomic coordinates for non-hydrogen atoms ($\times 10^4$) and for hydrogen atoms ($\times 10^3$) and equivalent isotropic thermal parameters ($U_{eq} = (U_{11} \times U_{22} \times U_{33})^{1/3} \times 10^4$; $u_{iso} \times 10^3$).

Atom	Site symmetry	SOF‡	x	y	z	U_{eq} (Å)^2
Al(1)	$\bar{3}$	1/6	0	5000	0	150(3)
Al(2)	$\bar{3}$	1/6	0	5000	5000	150(3)
F(1)	1	1	277(1)	6251(1)	235(1)	245(4)
F(2)	1	1	211(1)	6258(1)	4737(1)	258(5)
C	1	1	−2329(1)	7516(1)	5285(2)	273(7)
N(1)	1	1	−1388(1)	7514(1)	5248(1)	399(8)
N(2)	1	1	−2796(1)	8320(1)	5443(1)	384(6)
N(3)	1	1	−2783(1)	6688(1)	5175(1)	390(6)
H(1)	1	1	−107(2)	802(2)	531(1)	40(6)iso
H(1)*	1	1	−101	814	534	
H(2)	1	1	−108(2)	693(2)	518(2)	66(7)iso
H(2)*	1	1	−102	688	513	
H(3)	1	1	−339(2)	835(1)	542(1)	35(5)iso
H(3)*	1	1	−353	832	548	
H(4)	1	1	−250(1)	879(2)	546(2)	59(8)iso
H(4)*	1	1	−242	895	553	
H(5)	1	1	−331(2)	668(2)	516(2)	38(6)iso
H(5)*	1	1	−352	667	520	
H(6)	1	1	−232(2)	623(2)	506(2)	78(9)iso
H(6)*	1	1	−240	607	506	

* Calculated H atom positions used in the NMR calculation, assuming N–H bond equal to 1.03 Å and H–N–H angle equal to 120°.
‡ Site occupancy factor (SOF).

refined. The maximum shift/error for a parameter in the last cycles of refinement was 0.003. The final difference Fourier map showed electron density within a range of 0.25 to −0.60 e Å^{-3}. In the final stage of refinement, an isotropic extinction parameter x was included and refined to the value of 0.0464: F_c is multiplied by $(1 - 0.0001xF_c^2/\sin\theta)$. All calculations were carried out on an IBM XT/PC computer using the CRYSRULER package (Rizzoli *et al* 1986).

The final positional and thermal parameters are listed in tables 1 and 2 and bond lengths and angles in table 3. A structure factor table has been deposited with the British Library†.

2.4. *Discussion*

The symmetry of the crystal structure of the guanidinium hexafluoroaluminate, $P2_1/a\bar{3}$, causes significant changes in the ideal symmetry of the guanidinium cation, $\bar{6}m2$ (D_{3h}), and the $(AlF_6)^{3-}$ anion, $m\bar{3}m$ (O_h). Unlike in other guanidinium salts, $C(NH_2)_3ClO_4$ (Pająk *et al* 1982), $C(NH_2)_3BF_4$ (Kozak *et al* 1987) and $C(NH_2)_3PF_6$ (Grottel *et al* 1989), the guanidinium cation does not show any symmetry and the AlF_6^{3-} exhibits only $\bar{3}$ (C_6) symmetry. As a consequence, all guanidinium atoms are in general position (24d)

† Supplementary material of this paper contains a list of structure factors deposited in the British Library Publication Special Acquisitions. Copy may be obtained from the British Library Document Supply Centre, Boston Spa, Wetherby, Yorkshire, LS23 7BQ, UK.

Table 2. Anisotropic thermal parameters ($\times 10^4$) for non-hydrogen atoms. The temperature factor is of the form:

$$\exp[-2\pi^2(U_{11}h^2a^{*2} + U_{22}k^2b^{*2} + U_{33}l^2c^{*2} + 2U_{12}hka^*b^* + 2U_{13}hla^*c^* + 2U_{23}klb^*c^*)].$$

Atom	U_{11}	U_{22}	U_{33}	U_{12}	U_{13}	U_{23}
Al(1)	147(6)	147(6)	147(6)	−15(8)	−15(8)	−15(8)
Al(2)	153(6)	153(6)	153(6)	11(8)	11(8)	11(8)
F(1)	257(7)	190(8)	285(8)	−20(4)	−6(4)	−17(4)
F(2)	289(7)	190(8)	297(8)	18(4)	20(4)	−10(4)
C	228(12)	236(12)	353(13)	33(6)	−20(10)	−23(6)
N(1)	238(12)	248(12)	710(14)	−14(6)	27(9)	−34(6)
N(2)	260(10)	248(10)	642(12)	−23(8)	61(8)	25(8)
N(3)	230(10)	296(10)	647(13)	−19(8)	−12(8)	−32(8)

Table 3. Interatomic distances (Å) and angles (deg) with their ESD in parentheses.

C–N(1)	1.313(2)	N(1)–C–N(2)	120.3(1)
C–N(2)	1.316(2)	N(1)–C–N(3)	118.2(1)
C–N(3)	1.328(2)	N(2)–C–N(3)	121.5(1)
N(1)–H(1)	0.84(2)	C–N(1)–H(1)	121(2)
N(1)–H(2)	0.93(2)	C–N(1)–H(2)	118(2)
N(2)–H(3)	0.83(2)	H(1)–N(1)–H(2)	121(2)
N(2)–H(4)	0.77(2)	C–N(2)–H(3)	122(1)
N(3)–H(5)	0.75(2)	C–N(2)–H(4)	118(1)
N(3)–H(6)	0.91(2)	H(3)–N(2)–H(4)	119(2)
Al(1)–F(1)	1.818(1)	C–N(3)–H(5)	120(2)
Al(2)–F(2)	1.817(1)	C–N(3)–H(6)	107(2)
F(1) · · · F(1)	2.580(2)	H(5)–N(3)–H(6)	133(2)
F(1) · · · F(1)	2.561(2)	F(1)–Al(1)–F(1)	90.42(8)
F(2) · · · F(2)	2.577(2)	F(1)–Al(1)–F(1)	180.00(9)
F(2) · · · F(2)	2.562(2)	F(2)–Al(2)–F(2)	90.34(8)
		F(2)–Al(2)–F(2)	180.00(9)

and Al atoms occupy two inequivalent positions (4a) $(\frac{1}{2},\frac{1}{2},\frac{1}{2}; 0,\frac{1}{2},0; \frac{1}{2},0,0; 0,0,\frac{1}{2})$ and (4b) $(0,0,0; \frac{1}{2},0,\frac{1}{2}; 0,\frac{1}{2},\frac{1}{2}; \frac{1}{2},\frac{1}{2},0)$, having different molecular environments. Two of the C–N bonds are relatively short and very close to the C–N bonds found in $C(NH_2)_3PF_6$ of 1.314(4) Å (Grottel *et al* 1989). The third bond C–N(3) is significantly longer (table 3) and its lengthening was confirmed by Raman spectroscopy, revealing peaks at 1018 and 1026 cm^{-1} corresponding to two modes of the C–N stretching vibrations. The C–N(3) bond exhibits also angular deviations from C_3 symmetry around the C atom. The N(1)–C–N(3) and N(2)–C–N(3) angles differ from 120° about 15σ to 18σ. All the changes in the ideal symmetry of the guanidinium cation may be caused by a different H-bond pattern in each of the NH_2 groups involved. Only the non-hydrogen atoms of the guanidinium cation are planar with $\chi^2 = 3.83$ at 95% probability. The H atoms deviate significantly from planarity and $d/\sigma = 3.7$ for H(3) is the largest, where d is the distance of the atom from the least-squares plane.

The Al(1)–F(1) and Al(2)–F(2) distances of 1.818(1) Å and 1.817(1) Å in the two inequivalent hexafluoroaluminate anions are equal within experimental error. The same

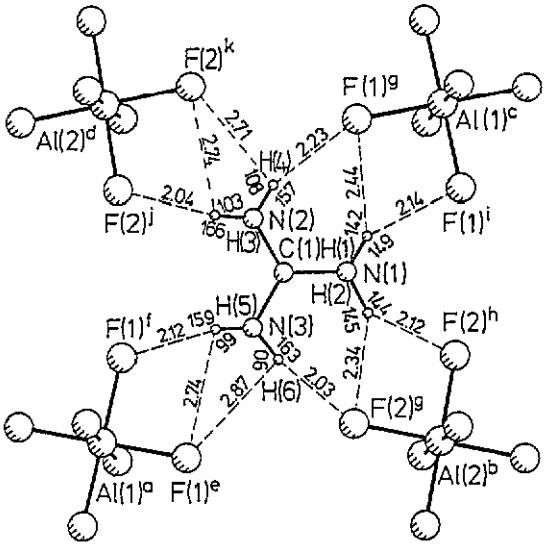

Figure 1. The hydrogen-bond pattern of $[C(NH_2)_3]_3AlF_6$. $\sigma(H\cdots F) = 0.02$ Å, $\sigma(N\text{–}H\cdots F) = 2°$. Symmetry codes are: (a) $-\frac{1}{2},\frac{1}{2},\frac{1}{2}$; (b) $0,\frac{1}{2},\frac{1}{2}$; (c) $0,1,\frac{1}{2}$; (d) $-\frac{1}{2},1,\frac{1}{2}$; (e) $y-1,-z+\frac{1}{2},x+\frac{1}{2}$; (f) $x-\frac{1}{2},y,-z+\frac{1}{2}$; (g) $-y+\frac{1}{2},-z+1,x+\frac{1}{2}$; (h) none; (i) $1+x,\frac{3}{2}-y,\frac{1}{2}+z$; (j) $x-\frac{1}{2},-y+\frac{3}{2},-z+1$; (k) $y-1,-z+\frac{3}{2},x+\frac{1}{2}$.

is true for F–Al–F angles (table 3). The deviations from the ideal $m\bar{3}m$ anion symmetry are about 9σ for F(1) $\cdots$ F(1) distances and 5σ for F(1)–Al(1)–F(1) angles. The corresponding values in the anion (2) are 7σ and 4σ.

There are 24 guanidinium cations and eight AlF_6 anions in the unit cell. Each cation is surrounded by four AlF_6 and each anion by 12 cations. The pattern of H bonds is given in figure 1. All H atoms in the NH_2 groups participate as double donors forming bifurcated H bonds, where one is a stronger and more linear N–H $\cdots$ F hydrogen bond with the H $\cdots$ F distance in the range of 2.04 to 2.14 Å and N–H $\cdots$ F angle in a range of 144° to 166°. The second bond is a relatively weak H-bond interaction. Each F(1) atom from anion (1) and F(2) from anion (2) is involved in six H-bond interactions. The stereo view of a unit cell content is given in figure 2. The molecular packing can be described as a framework of AlF_6 ions (where Al atoms occupy octahedral voids) H-bonded with guanidinium cations lying approximately parallel to (100) planes.

3. NMR investigation

3.1. Experimental details

The guanidinium hexafluoroaluminate $[C(NH_2)_3]_3AlF_6$ was obtained following the reaction (Szczepański 1990):

$$3[C(NH_2)_3]_2CO_3 + 2Al(OH)_3 + 12HF \rightarrow 2[C(NH_2)_3]_3AlF_6 + 3CO_2 + 9H_2O.$$

The substrates were treated with an excess of hydrofluoric acid (40% aqueous solution) and heated to complete dissolution. After cooling, beautiful small cubes of

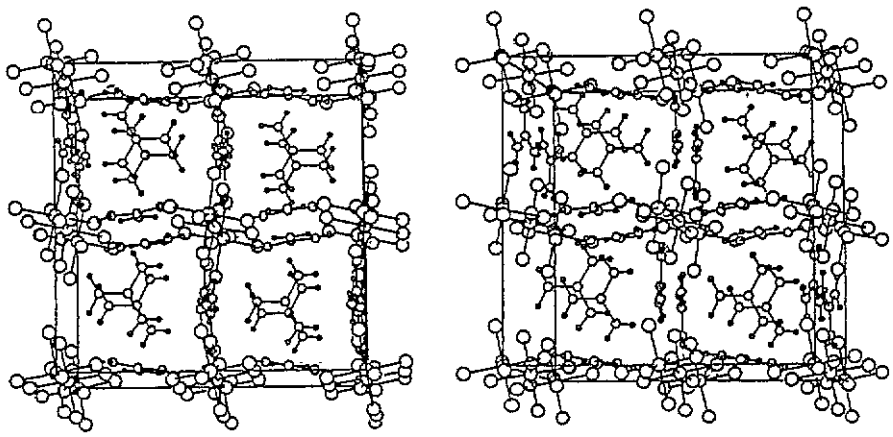

Figure 2. Stereoscopic view of the unit cell content.

$[C(NH_2)_3]_3AlF_6$ crystals were obtained†. To remove iron paramagnetic impurities revealed in the crystals by electron paramagnetic resonance (EPR) purity control, the compound was recrystallized from 20% solution of hydrofluoric acid with a small amount of tartaric acid added. The product was then ground to a powder, dried, degassed and sealed off.

Measurements of proton and fluorine NMR second moments (accuracy ±5%) were performed from 100 to 513 K by means of a wide-line spectrometer, operating at Larmor frequencies of 28.0 and 26.3 MHz, for protons and fluorines, respectively. The second moment values were calculated by a numerical integration of the first derivatives of absorption lines and corrected for finite modulation amplitude (Andrew 1953). Mean values were obtained for about four derivatives registered at each temperature. Measurements of proton and fluorine spin–lattice relaxation times (accuracy ±7%) were performed as a function of temperature with a 40 MHz pulse spectrometer by a $\pi/2$—τ—$\pi/2$ pulse sequence or by a saturation method.

The temperature of the sample was controlled by means of a gas-flow cryostat and monitored with a Pt resistor to an accuracy of 1 K. All measurements were taken with increasing temperature.

Differential thermal analysis (DTA) was carried out with Derivatograph type OD 102 system, from Hungary.

3.2. Results

Results of the proton and fluorine NMR second moment studies performed as a function of temperature are shown in figure 3. The proton second moment value of about 26 G^2 observed at low temperature starts to decrease slowly at 210 K and then sharply at 270 K to about 5 G^2, achieved above 395 K. At temperatures higher than 210 K a small narrow line is observed in the middle of each curve (see figure 3). The fluorine second moment value of 19.4 G^2 registered at low temperature starts to diminish at 210 K to 11 G^2, observed at 323 K. Then its value slowly decreases to 9.3 G^2 at 433 K and thereafter more sharply to 1.7 G^2, achieved at 513 K.

† Another synthesis of the compound was described by Bukovec (1983)

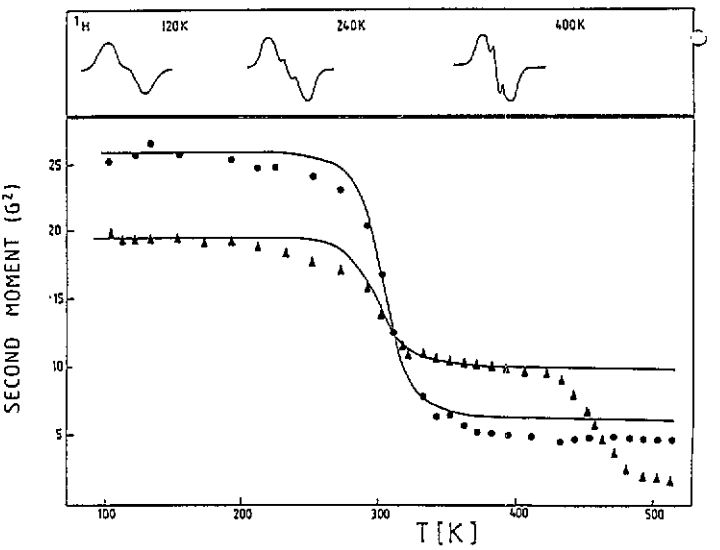

Figure 3. Temperature dependence of ^1H (●) and ^{19}F (▲) NMR second moments and the shapes of ^1H resonance-line derivatives. Full curves are theoretically calculated for the C_3 reorientation of the guanidinium cation.

The results of the proton and fluorine spin–lattice relaxation times are shown as log T_1 plots against inverse temperature in figures 4 and 5, respectively. The curves in the figures are theoretical fits to the experimental data. At all the temperatures studied, a non-exponential proton and fluorine magnetization decay is observed. The decay curves are decomposed into two exponential terms with different T_1 values, yielding the results shown in figures 4 and 5. For both ^1H and ^{19}F nuclei one can see T_1 minima of 14 ms at about 385 K revealed in the plots of their short components. At low temperature a non-typical behaviour of ^1H and ^{19}F relaxation times connected with a change in respective magnetization amplitudes is observed. On figures 4 and 5 the full circles and triangles denote T_1 components for magnetization amplitudes higher than 0.5. The temperature behaviour of experimental magnetization amplitudes of short and long T_1 components observed in the ^1H experiment is shown in figure 6. The full and broken curves are theoretical fits to the experimental values of the amplitudes.

A DTA study performed from room temperature to 620 K revealed that the compound started to decompose at about 580 K. No solid–solid phase transition was found in this temperature range.

3.3. Calculations and discussion

3.3.1. NMR second moment. The theoretical proton and fluorine second moment values for the rigid structure of the compound were found numerically using our x-ray data and the Van Vleck (1948) formula. Contributions from all kinds of magnetic nuclei occurring in the sample were taken into account. Since an x-ray study does not reveal precise hydrogen atom positions (Schuster *et al* 1976), we assumed a normalized geometry of NH_2 group: N–H = 1.03 Å and H–N–H = 120°. Table 4 presents the proton and fluorine second moment values obtained. As one can see, the structural inequivalence of the

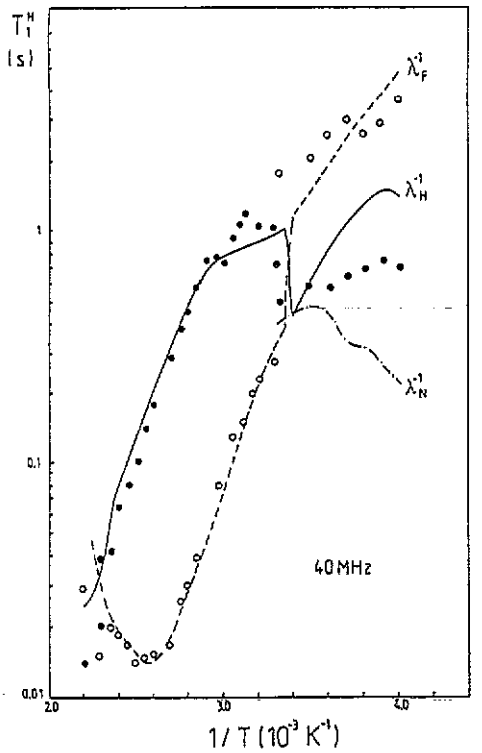

Figure 4. Temperature dependence of the proton spin–lattice relaxation time: (●) components for magnetization amplitude higher than 0.5.

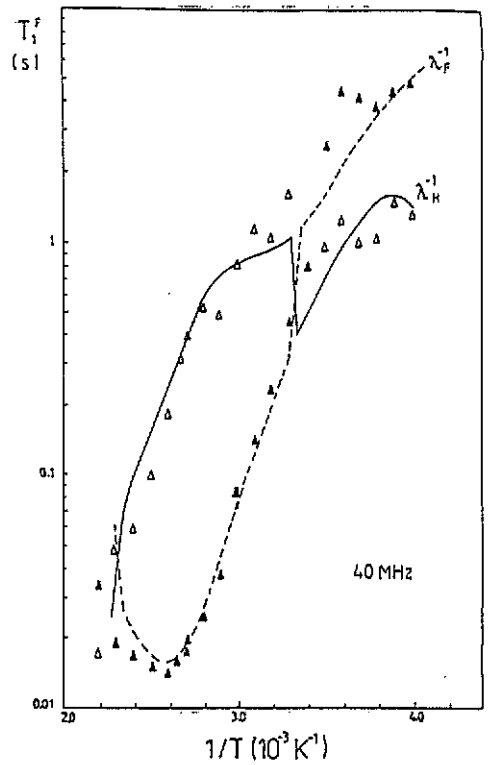

Figure 5. Temperature dependence of the fluorine spin–lattice relaxation time: (▲) components for magnetization amplitude higher than 0.5.

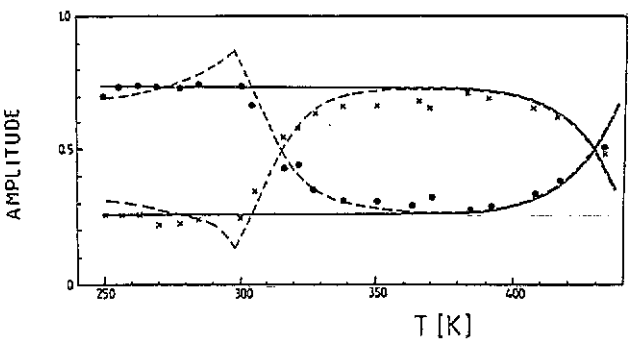

Figure 6. Temperature dependence of magnetization amplitudes of T_1^H long (×) and short components (●) and the theoretical plots calculated for C_3 reorientation of the guanidinium cation (———) and for C_3 reorientation preceded by NH_2 motion (– – – –).

anions leads to somewhat different values of their second moments. The mean value for both anions (19.78 G^2) agrees very well with the experimental 19.4 G^2 registered at low temperature. Similarly, for protons, a very good agreement between the theoretical and

Table 4. Second moment values calculated for the rigid structure of $[C(NH_2)_3]_3AlF_6$.

Interaction	$M_2(^1H)$ (G^2)	Interaction	$M_2(^{19}F)$ (G^2)	
			$AlF_6(1)$	$AlF_6(2)$
H–H	20.64	F–F	4.88	4.82
H–N	1.88	F–Al	3.48	3.44
H–F	3.50	F–H	10.79	12.11
H–Al	0.14	F–N	0.02	0.02
	26.16		19.17	20.39

experimental values (~26 G^2) at low temperature was obtained. It means that at those temperatures both ion sublattices are rigid on the NMR timescale.

On increase in temperature the proton and fluorine second moments are evidently reduced, which can be accounted for by the onset of ion motions in the crystal lattice. To explain the nature of these motions, we calculated the reduced second moment values for various models of reorientations. Similarly as in the other guanidinium salts, we could ascribe the one-step reduction of the proton second moment to a C_3 reorientation of the guanidinium cation around the symmetry axis perpendicular to the cation plane†. The theoretical proton second moment value reduced by this reorientation should be equal to 6.4 G^2. Taking this value into account and using the BPP formula (Bloembergen *et al* 1948) as well as the activation parameters from our relaxation study, we found a theoretical plot of the second moment as a function of temperature (figure 3). A comparison with the experimental data implies that the C_3 reorientation is preceded by another motion. It is difficult to say what kind of motion it is. The slight diminishing of the proton second moment observed between 210 and 270 K probably reflects the onset of the NH_2 group motion taking place in the guanidinium cation. The narrow line appearing above 210 K in the middle of the proton spectrum seems to confirm this reorientation. The motion of one NH_2 group followed by C_3 reorientation of the cation seems to be insufficient to explain the experimental proton second moment value (~5 G^2) found at the highest temperatures. The onset of the second NH_2 group reorientation hindered by a higher energy barrier could probably take place at higher temperatures. The activation energy for the motion of the first NH_2 group estimated from the formula of Waugh and Fiedin (1962) equals about 29 kJ mol^{-1}. The onset of the second NH_2 group should require a much higher activation energy. The theoretical considerations of the rotational barriers in the 'Y-aromatic' guanidinium ion (Bally *et al* 1975, Capitani and Pederson 1978, Sapse and Massa 1980) have shown that a rotation of the second NH_2 group must be energetically more costly, since after onset of the first group the remaining C–N bonds not involved in the rotation become more strongly π-bonded than before. An interesting feature of the compound studied is that each NH_2 group of the guanidinium cation is involved in different hydrogen bonds N–H · · · F. Thus different local potentials make three amino groups dynamically inequivalent.

It is surprising that the first step of the fluorine second moment reduction to about 11 G^2 cannot be reasonably explained by the onset of any reorientation of the anions.

† A deviation from C_3 symmetry of the cation revealed by our X-ray analysis can be neglected from the NMR point of view.

Our calculations presented as the full curve in figure 3 show that this value evidently results from the modulation of the dominant fluorine–proton interaction (see table 4) by the guanidinium cation reorientations. The deviation of the fluorine experimental results from the theoretical plot between 210 and 270 K (figure 3) further confirms the onset of the NH_2 group modulating the strong H–F interaction. Above 323 K the slight diminishing of ^{19}F second moment to 9.3 G^2 may reflect the onset of the second NH_2 group motion. The next step of marked reduction of ^{19}F second moment to 1.7 G^2 reveals as late as at 433 K the onset of an isotropic anion reorientation. Noteworthy is a high activation energy for the anion motion in this compound. The value of about 67 kJ mol^{-1} estimated from the Waugh–Fiedin formula is much higher than the respective value for the cation reorientation of about 44 kJ mol^{-1}.

Taking the difference in crystallographic environment of the two anions (1) and (2) into account, one could expect their different mobilities and thus different activation energies, similarly as found in $C(NH_2)_3PF_6$. The reason that we do not see any dynamic inequivalence of both anions is that when the AlF_6 anions start to reorient the motion of the guanidinium cation is already set in and the F–H interaction is reduced to a great extent.

3.3.2. NMR relaxation. The temperature dependence of the component of the ^1H spin–lattice relaxation time representing the main contribution to the proton magnetization (full circles in figure 4) does not reveal the expected minimum corresponding to the C_3 reorientation of the guanidinium cation. However, the activation energy of 45 kJ mol^{-1} determined from the slope of the log T_1 versus $1/T$ plot agrees well with the value estimated for this reorientation from our second moment study. On the other hand, the minimum observed for the component of ^{19}F spin–lattice relaxation time representing the main contribution to the fluorine magnetization (full triangles in figure 5) cannot be explained as arising from any reorientation of the anions. The activation energy value obtained from the respective slope for ^{19}F is the same as for protons. It strongly suggests that the minimum must be related to the dynamics of the cation through the heteronuclear proton–fluorine interaction $\tau_c \simeq (\omega_H - \omega_F)^{-1}$. The experimental non-exponential behaviour of T_1^H and T_1^F is typical for a cross-relaxation effect in a multi-spin system. As the compound studied contains not only ^1H and ^{19}F spins but also two others, ^{27}Al and ^{14}N, one must consider a cross-relaxation effect in a system of four unlike spins, as we did previously (Grottel *et al* 1989).

To describe the time behaviour of the proton and fluorine magnetizations, we calculated relaxation matrix elements for the assumed model of the guanidinium cation motions. As it results from our second moment study we have considered the C_3 reorientation of the cation preceded by a motion of one NH_2 group, while the anions are still rigid. Hence the following relaxation matrix should be considered:

$$R = R_{NH_2} + R_{C_3}$$

where R_{NH_2} and R_{C_3} correspond to the motions mentioned above.

To calculate diagonal (R_{II}) and off-diagonal (R_{IS}) elements of the relaxation matrix, the following formulae were used:

$$R_{II} = \tfrac{2}{3}\gamma_I^2 \Delta M_2^{II} g_1(\omega_I, \tau) + \tfrac{1}{2} \sum_S \gamma_I^2 \Delta M_2^{IS} g_2(\omega_I, \omega_S, \tau)$$

$$R_{IS} = \tfrac{1}{2}\gamma_S^2 \Delta M_2^{SI} g_3(\omega_I, \omega_S, \tau) N_S/N_I$$

where

$$g_1(\omega_I, \tau) = \tau/(1 + \omega_I^2\tau^2) + 4\tau/(1 + 4\omega_I^2\tau^2)$$

$$g_2(\omega_I,\omega_S,\tau)=\tau/[1+(\omega_I-\omega_S)^2\tau^2]+3\tau/(1+\omega_I^2\tau^2)+6\tau/[1+(\omega_I+\omega_S)^2\tau^2]$$

$$g_3(\omega_I,\omega_S,\tau)=-\tau/[1+(\omega_I-\omega_S)^2\tau^2]+6\tau/[1+(\omega_I+\omega_S)^2\tau^2].$$

Here τ denotes a correlation time of the C_3 reorientation of the whole cation or of the NH_2 group motion.

Using our x-ray data we calculated for the C_3 reorientation the contributions to the reduction of the second moment values as follows: ΔM_2(H–H) = 15.5 G^2, ΔM_2(H–N) = 1.6 G^2, ΔM_2(H–F) = 2.7 G^2 and ΔM_2(H–Al) = 0.04 G^2. For the NH_2 group motion we could only estimate the respective values, obtaining: ΔM_2(H–H) = 0.5 G^2, ΔM_2(H–F) = 0.5 G^2 and ΔM_2(H–N) = 0.3 G^2.

Assuming an Arrhenius dependence of the correlation times, we calculated the relaxation matrix R and its eigenvalues λ_H, λ_F, λ_N and λ_{Al}. The inverses λ_H^{-1} and λ_F^{-1} were then compared with the respective experimental T_1^H and T_1^F values (figures 4 and 5), giving a good agreement at high temperatures. It proves that the relaxation in this temperature region is mainly due to the C_3 reorientation of the guanidinium cation. At low temperature the calculated λ_H^{-1} and λ_F^{-1} values correspond qualitatively to the experimental results. Better agreement could not be obtained since the relaxation rate for the NH_2 group motion could be only roughly estimated. Another reason is that it was not possible to decompose the proton magnetization time dependence into three components (λ_H^{-1}, λ_F^{-1} and λ_N^{-1}) found in our calculations. It should also be mentioned that in the whole temperature range the ^{27}Al contribution to the proton and fluorine magnetizations can be neglected. A significant shortening of the main contribution to the proton relaxation at about 300 K evidently reflects the existence of NH_2 group motion.

To explain the non-typical behaviour of the relaxation times, we have undertaken a detailed analysis of the temperature dependence of magnetization amplitudes. The analytical solution of the set of coupled differential equations describing the time variations of nuclear magnetizations for a system of four unlike spins (Grottel *et al* 1989) enabled us to derive magnetization amplitudes of the short and long components of the relaxation times for the assumed model of reorientation as a function of temperature. The results obtained for the proton magnetization are presented in figure 6. Assuming only C_3 reorientation of the guanidinium cation, the amplitude ratio should be constant up to about 400 K, and above this temperature one should expect an inversion of their values. Taking into account C_3 reorientation preceded by NH_2 group motion, one obtains drastically different behaviour of both amplitudes, namely one should observe the second inversion point at low temperature. Our experimental data agree very well with the latter model of the motion, thus evidently confirming the existence of another motion except C_3 reorientation of the cation.

The best-fitted activation parameters obtained for both types of reorientation are presented in table 5. The activation energy for C_3 reorientation of the guanidinium

Table 5. Activation parameters for the motions considered.

	E_a (kJ mol^{-1})	τ_0 (s)
C_3 reorientation	44.9	5.80×10^{-14}
NH_2 reorientation	27.2	6.07×10^{-14}

cation in hexafluoroaluminate, 44.9 kJ mol^{-1}, is comparable with the values of 37.7 and 43.2 kJ mol^{-1} found in tetrafluoroborate and hexafluorophosphate. A striking difference is however observed in the dynamic behaviour of anions in those compounds. The energy barriers 20.5 and 25 kJ mol^{-1} for $C(NH_2)_3BF_4$ and $C(NH_2)_3PF_6$, respectively, are much lower than found for the cations. The situation is inversed for the compound under study, where the hindering barrier for the anion (only estimated from the second moment study) is much higher than for the cation. It results from the greater number of hydrogen bonds in which each anion is involved compared with the cation.

Acknowledgment

This research was supported by the Polish Academy of Sciences under Project CPBP 01.12.

References

Andrew E R 1953 *Phys. Rev.* **91** 425
Bally T, Diehl P, Haselbach E and Tracey A S 1975 *Helv. Chim. Acta* **58** 2398
Bloembergen N, Purcell E M and Pound R V 1948 *Phys. Rev.* **73** 679
Bukovec P 1983 *Monatsh. Chem.* **114** 277
Capitani J F and Pederson L 1978 *Chem. Phys. Lett.* **54** 547
Gima S, Furukawa Y and Nakamura D 1984 *Ber. Bunsenges. Phys. Chem.* **88** 939
Grottel M, Kozak A, Kozioł A E and Pająk Z 1989 *J. Phys.: Condens. Matter* **1** 7069
Grottel M and Pająk Z 1984 *J. Chem. Soc. Faraday Trans. II* **80** 553
Jaskólski M 1982 *Collected Abstracts, 4th Symp. Organic Crystal Chemistry* (Poznań) p 70
Kozak A, Grottel M, Kozioł A E and Pająk Z 1987 *J. Phys. C: Solid State Phys.* **20** 5433
Lehman M S and Larsen F K 1974 *Acta Crystallogr.* A **30** 580
Pająk Z, Grottel M and Kozioł A E 1982 *J. Chem. Soc. Faraday Trans. II* **78** 1529
Pająk Z, Kozak A and Grottel M 1988 *Solid State Commun.* **65** 671
Ratcliffe C I 1985 *Can. J. Chem.* **63** 1239
Rizzoli C, Sangermano V, Calestani G and Andreetti G D 1986 *CRYSRULER Package* Parma, Italy
Sapse A M and Massa L J 1980 *J. Org. Chem.* **45** 719
Schuster P, Zundel G and Sandorfy C 1976 *The Hydrogen Bond* (Amsterdam: North-Holland)
Sheldrick G M 1986 *SHELXS-86 Program for Crystal Structure Determination* Göttingen, Germany
Szczepański W 1990 unpublished data
Van Vleck J H 1948 *Phys. Rev.* **74** 1168
Waugh J S and Fiedin E I 1962 *Fiz. Tverd. Tela* **4** 2233